Citation: Molecular Therapy—Nucleic Acids (2016) 5, e280; doi:10.1038/mtna.2015.51
Official journal of the American Society of Gene & Cell Therapy

www.nature.com/mtna

Silencing CCR2 in Macrophages Alleviates Adipose Tissue Inflammation and the Associated Metabolic Syndrome in Dietary Obese Mice

Jongkil Kim[1], Kunho Chung[1,2], Changseon Choi[1,2], Jagadish Beloor[2], Irfan Ullah[1], Nahyeon Kim[1], Kuen Yong Lee[1], Sang-Kyung Lee[1] and Priti Kumar[2]

Adipose tissue macrophage (ATM)-mediated inflammation is a key feature contributing to the adverse metabolic outcomes of dietary obesity. Recruitment of macrophages to obese adipose tissues (AT) can occur through the engagement of CCR2, the receptor for MCP-1 (monocyte chemoattractant protein-1), which is expressed on peripheral monocytes/macrophages. Here, we show that i.p. administration of a rabies virus glycoprotein-derived acetylcholine receptor-binding peptide effectively delivers complexed siRNA into peritoneal macrophages and ATMs in a mouse model of high-fat diet-induced obesity. Treatment with siRNA against CCR2 inhibited macrophage infiltration and accumulation in AT and, therefore, proinflammatory cytokines produced by macrophages. Consequently, the treatment significantly improved glucose tolerance and insulin sensitivity profiles, and also alleviated the associated symptoms of hepatic steatosis and reduced hepatic triglyceride production. These results demonstrate that disruption of macrophage chemotaxis to the AT through cell-targeted gene knockdown strategies can provide a therapeutic intervention for obesity-related metabolic diseases. The study also highlights a siRNA delivery approach for targeting specific monocyte subsets that contribute to obesity-associated inflammation without affecting the function of other tissue-resident macrophages that are essential for host homeostasis and survival.

Molecular Therapy—Nucleic Acids (2016) **5**, e280; doi:10.1038/mtna.2015.51; published online 26 January 2016
Subject Category: siRNA, shRNAs and miRNAs; Therapeutic proof-of-concept

Introduction

Obesity in humans is accompanied by inflammation and a major associative risk for the "metabolic syndrome," which is a collection of pathological states including resistance to insulin, hyperglycemia, hypertension, and dyslipidemia leading to diseases such as type 2 diabetes, cardiovascular disease, hepatic steatosis, airway disease, neurodegeneration, biliary disease, and certain cancers.[1–5] Recent advances in obesity research have unearthed that the low-grade but chronic inflammation developing on account of excess nutrient uptake in metabolic tissues such as the liver, skeletal muscle, and adipose tissue (AT) is an important connecting link between obesity and insulin resistance.[4,6,7] In both rodents and humans, it is now well recognized that macrophages that infiltrate and accumulate in the visceral AT depot during obesity are a critical component of the inflammatory cell milieu.[8–10] Adipose tissue macrophage (ATM) numbers also correlate with systemic insulin resistance in obese human subjects.[11,12] ATMs, polarized to the M1 or "classically activated inflammatory" state, that predominate in obese visceral AT, produce proinflammatory cytokines such as tumor necrosis factor-α (TNF-α), interleukin-6 (IL-6), and inducible nitric oxide synthase.[13–15] This is believed to impair adipocyte ability to secrete beneficial adipokines or store lipid, leading to ectopic lipid deposition in the liver and muscle, a causal factor for insulin resistance.[16–18] In contrast, M2 or "alternatively activated noninflammatory" macrophages that predominate in normal or lean AT may promote a reduced inflammatory environment by secreting suppressive cytokines like arginase-1 and IL-10.[19,20] Diet-induced obesity polarizes ATMs from an M2 to M1 proinflammatory state.[15,21] Thus, interventions that disrupt macrophage recruitment into the AT, block M1-polarization of macrophages, and/or attenuate AT inflammation may alleviate the metabolic syndrome associated with obesity.[22,23]

In obese mice, increased levels of monocyte chemoattractant protein-1 (MCP-1) (also called chemokine (C-C motif) ligand 2 or CCL2) in the AT are strongly associated with increased infiltration and accumulation of ATMs expressing CCR2, the MCP-1 receptor.[24–29] Increased levels of MCP-1 in plasma and subcutaneous AT and elevated levels of CCR2-expressing inflammatory cells in AT of obese human subjects are strongly associated with insulin resistance.[24,28–32] These observations implicate MCP-1 in the recruitment of macrophages to the AT and in the development of insulin resistance in obese humans and rodents through similar mechanisms. Mice deficient in CCR2 display lower inflammation in AT and have a reduced propensity to develop insulin resistance while mice overexpressing MCP-1 have an exacerbated insulin resistance phenotype.[24,25,29,32] CCR2 is also a receptor for other chemokines such as CCL7 (MCP-3), CCL8 (MCP-2),

[1]Department of Bioengineering and Institute of Nanoscience and Technology, Hanyang University, Seoul, Korea; [2]Department of Internal Medicine, Section of Infectious Diseases, Yale University School of Medicine, New Haven, Connecticut, USA. Correspondence: Priti Kumar, Department of Internal Medicine, Section of Infectious Diseases, Yale University School of Medicine, 25 York Street, New Haven, Connecticut 06510, USA. E-mail: priti.kumar@yale.edu or Sang-Kyung Lee, Department of Bioengineering and Institute of Nanoscience and Technology, Hanyang University, Haengdong-1 dong, Seongdong-gu, Seoul 133-791, Korea. E-mail: sangkyunglee@hanyang.ac.kr
Keywords: adipose tissue inflammation; CCR2; macrophage-targeted delivery; metabolic syndrome; obesity
Received 17 June 2015; accepted 23 November 2015; published online 26 January 2016. doi:10.1038/mtna.2015.51

CCL12 (MCP-5), and CCL13 (MCP-4) that are all increased in inflamed obese AT.[7,25,33] Thus, blockade/reduction of CCR2 expression in macrophages may disrupt their chemotaxis to the AT and reduce the downstream effects of obesity-induced inflammation.

siRNAs have immeasurable clinical potential, however their therapeutic value remains untapped mainly due to the hurdle of effective delivery *in vivo*.[34,35] We reported the use of cell-binding ligands attached to an arginine-rich cationic cell-penetrating peptide (9R) for the effective and targeted delivery of electrostatically complexed siRNA into cells *in vivo*.[36–38] One such ligand, RVG, a 32 amino acid peptide derived from the rabies virus envelope glycoprotein, binds nicotinic acetylcholine receptor (nAchR) subunits that are expressed on human and rodent monocytes/macrophages.[37,39,40] Here, we demonstrate that macrophage-targeted siRNA delivery using RVG for knockdown of CCR2 expression reduces macrophage infiltration into inflamed AT and consequently, the inflammatory response. The treatment induced widespread beneficial effects on the associated metabolic syndrome and improved systemic glucose tolerance, restored insulin sensitivity, and also ameliorated the accompanying symptoms of hepatic steatosis.

Results

Characterization of RVG9R3LC:siRNA complexes

The peptide used in this study, RVG9R3LC, was modified from its original sequence (RVG9R[37]) by the addition of three leucine and one cysteine residues at the carboxyl terminus, which enhanced cytoplasmic delivery (Lee, S-K unpublished data). To assess peptide interaction with negatively charged siRNA, RVG9R3LC was incubated with 100 pmol of siRNA at different molar excesses and the siRNA complexes formed analyzed by electrophoresis on a 1% agarose gel (**Figure 1a**). siRNA retardation commenced at a 5:1 peptide:siRNA ratio and was complete at 20:1 and higher. The peptide:siRNA complexes exhibited nanometer scale size distributions, with average particle diameters ranging from 107.0±1.76 to 172.07±1.60 nm between 10:1 and 80:1 peptide:siRNA molar ratios (**Figure 1b**). All complexes also recorded an overall positive charge with zeta potential ranging from 19.7 to 28.2 mV (**Figure 1c**). The smallest particle size (107.0±1.76 nm) recorded at a 40:1 peptide:siRNA was also the highest in positive zeta potential (28.23 mV), suggesting a tight association of the siRNA with the peptide at this ratio.

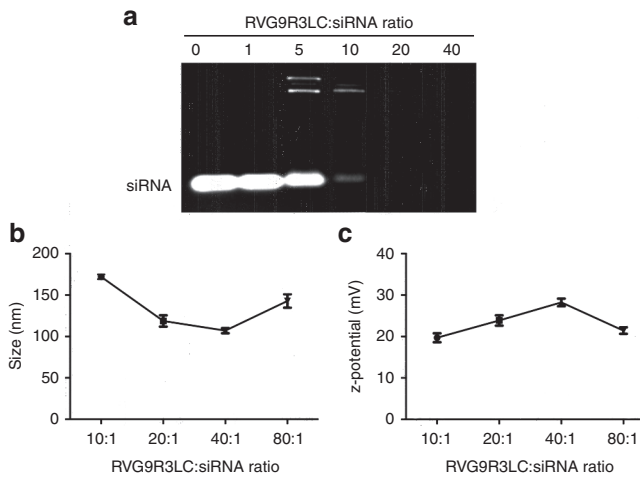

Figure 1 Physical characteristics of RVG9R3LC:siRNA complexes. (**a**) Electrophoretic gel mobility shift assays with 100 pmol siRNA complexed to RVG9R3LC at the indicated molar excesses of the peptide. (**b,c**) Average particle diametric size distribution in nanometer (Z_{Ave}) and surface charge distribution (ζ) of peptide-siRNA complexes (100 pmol siRNA) measured by dynamic light scattering. Error bars indicate SEM; $n = 3$.

RVG9R3LC mediates functional delivery of siRNA into murine macrophages

We assessed siRNA delivery by incubating Raw 264.7 cells, a murine monocytic cell line that expresses nAchR,[39] with RVG9R3LC complexed to FITC-labeled siRNA (siFITC). Significant transfection, in terms of numbers of cells as well as levels transfected per cell, occurred in a peptide:siRNA ratio-dependent manner (**Figure 2a**,**b**). A CCK-8-based cytotoxicity assay revealed slight toxicity only at the highest peptide:siRNA ratio (80:1), (**Supplementary Figure S1**). We therefore restricted our functional investigations to RVG9R3LC:siRNA complexes formed at a 40:1 molar ratio. Treatment of Raw 264.7 cells under these conditions with 100 pmol siRNA targeting CCR2 (siCCR2) induced an ~60% reduction in target mRNA levels (**Figure 2c**). Interestingly, Lipofectamine 2000 was ineffective in inducing knockdown, consistent with the known resilience of Raw 264.7 cells to nucleic acid transfection with this reagent.[41]

We next assessed whether RVG9R3LC can deliver siFITC into primary murine peritoneal macrophages that also express the nAchR.[39] Transfection efficiencies with RVG9R3LC:siFITC complexes were 90%, twice as high as those with Lipofectamine 2000 (**Figure 2d**,**e**). The amount of siRNA delivered per cell, reflected by mean fluorescence intensity, was also on average 30 times higher with RVG9R3LC (1047.7±56.4) than with Lipofectamine 2000 (36.1±2.8). The siRNA delivered was functional and resulted in an ~80% reduction in CCR2 mRNA levels with 100 pmol siRNA in comparison to the ~45% obtained with Lipofectamine (**Figure 2f**).

RVG9R3LC:siRNA complexes silence target gene expression in ATMs *in vivo*

We examined the biodistribution of i.p.-injected RVG9LR3C:siRNA complexes in obese mice maintained on a high-fat diet (HFD). For this, we used RVG9R3LC complexed to siFITC (0.1 mg/kg body weight) at a 40:1 ratio. Strong siRNA fluorescence was associated with $CD11b^+$ cells isolated from the peritoneal cavity and epididymal white adipose tissue (eWAT), and to a smaller with those from peripheral blood, but not with $CD11b^+$ cells in the spleen, lung, and liver (**Figure 3a**,**b**). The cell types targeted were $CD11b^+CD14^+$ macrophages and $CD11b^-$ or $CD11b^+CD14^-$ cells were not positive for siFITC suggesting that the i.p. route primarily targets peritoneal and eWAT macrophages (see **Figure 4b**). This is consistent with previous studies demonstrating localization of glucan shells (glucan-encapsulated siRNA particles), gold nanoparticles, clodronate liposomes, and basic

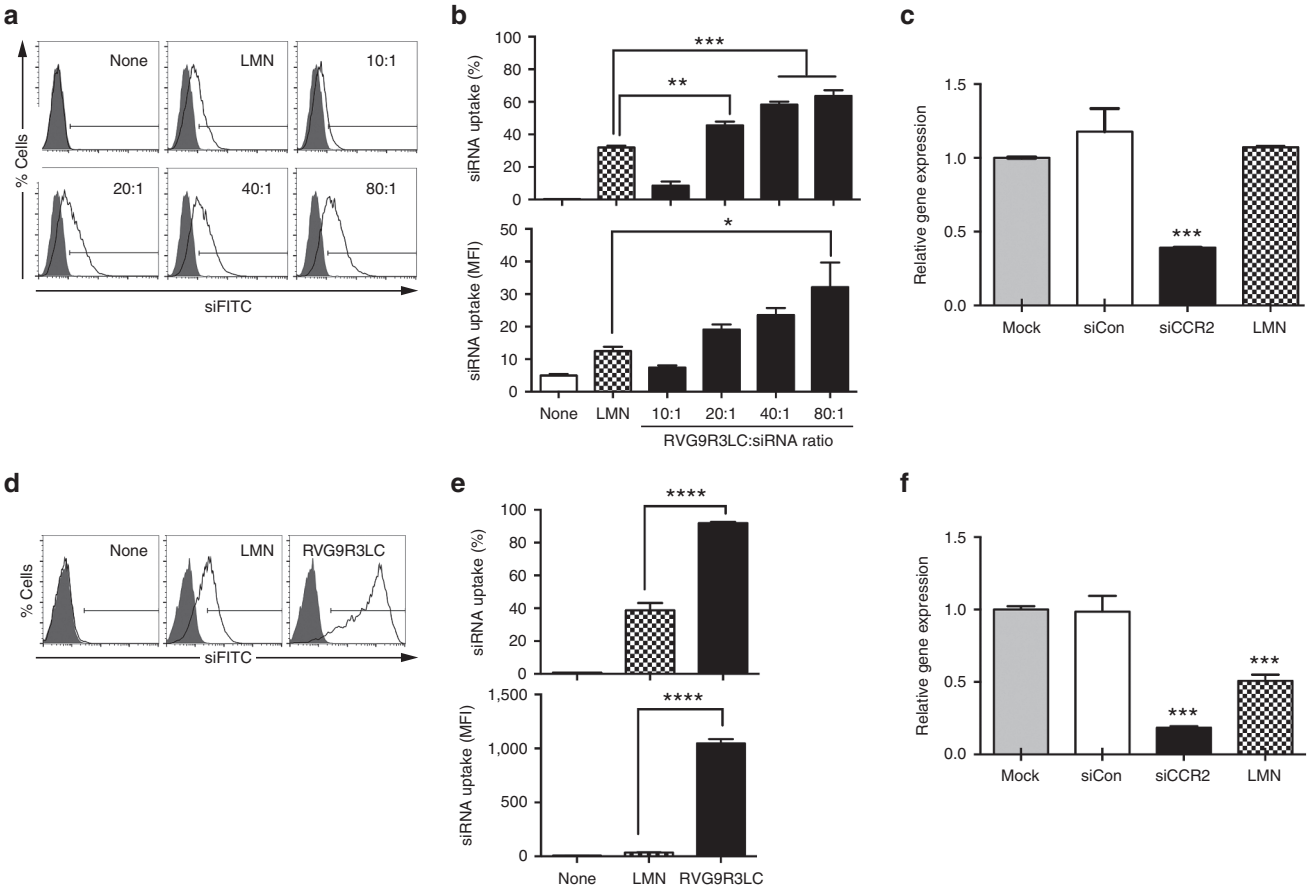

Figure 2 RVG9R3LC transfects siRNA into murine macrophages. Flow cytometric analysis of murine Raw 264.7 cells (**a,b**) and peritoneal cavity macrophages (**d,e**) 18 hours after exposure to RVG9R3LC:siFITC complexes. Representative histograms are shown in (a) and (**d**), and cumulative data for siRNA transfection efficiencies depicted as percent cells (upper panel) and mean fluorescence intensity (lower panel) in (**b** and **e**). Filled histograms in (**a** and **d**) represent nontreated cells (mock). In the upper panels of (**b**) and (**e**), cells were scored as positive for siRNA uptake using the marker gate (black line) depicted in (**a**) and (**d**), respectively. (**c,f**) Data presented are CCR2 mRNA levels after normalization to mGAPDH mRNA relative to that in untreated Raw 264.7 cells (**c**) and wild-type peritoneal macrophages (**f**) 24 hours after exposure to RVG9R3LC/siCCR2 complexes (100 pmol siRNA). Peptide:siRNA ratios are as indicated in (**a**) and (**b**) or 40:1 in (**c**) to (**f**). In all cases, error bars indicate SEM, $n = 3$. Significance was computed by analysis of variance and Bonferroni posttest, $^{*}P < 0.05$, $^{**}P < 0.01$, $^{***}P < 0.001$, $^{****}P < 0.0001$. LMN, Lipofectamine 2000; Mock, nontreated cells; None, no transfection reagent; siCon, siRNA targeting human CD4.

peptides and lipophilic drugs in AT but not in other organs, particularly upon i.p. injection.[42–47]

To evaluate CCR2 silencing, obese mice were treated with RVG9R3LC complexed with siCCR2 (0.1 mg/kg bodyweight) on alternate days for 6 weeks. We observed a reduction in CCR2-expressing CD11b macrophages from the peritoneum and eWAT and in addition, also in CD11b^{+} macrophages in the peripheral blood and liver (**Figure 3c**). CCR2 expression was reduced by as much as 60% in the eWAT in mice treated with RVG9R3LC complexed to siCCR2 when compared with mice treated with the peptide complexed to a nonspecific control siRNA. Expression of other macrophage cell markers like CD45, CD14, and CD11b remained unchanged confirming the specificity of target gene silencing. These data indicate that i.p. treatment with RVG9R3LC:siCCR2 over longer periods of time reduces the levels of CCR2^{+} macrophages not just in the peritoneum and eWAT but also in other inflamed tissues like the liver and peripheral blood. This is likely a consequence of reduced macrophage migration from the peritoneum and eWAT due to decreased CCR2 expression. Thus, reduced numbers of CCR2^{+} macrophages (**Figure 3d**, left) as well as lower levels of surface CCR2 expression per cell (measured as mean fluorescence intensities, **Figure 3d**, right) were recorded.

The use of a control nontargeting peptide RVM9R3LC, that binds siRNA similar to RVG9RLC (**Figure 4a**) but does not bind the nAchR,[37] also resulted in siFITC association with ATMs (and peritoneal macrophages), but at reduced levels when compared to RVG9R3LC (**Figure 4b**). However, minimal or no CCR2 silencing was observed (**Figure 4c**,**d**), suggesting that RVM9R3LC:siRNA uptake was mediated nonspecifically, through other mechanisms like phagocytic activity and not through peptide-mediated engagement of receptors, as in the case of RVG9R3LC, which is critical for functional delivery of siRNA into the cytoplasm.[38] This is in agreement with our previously published data that receptor engagement by a targeting peptide is critical for eliciting cytoplasmic localization of siRNA and silencing activity.[38]

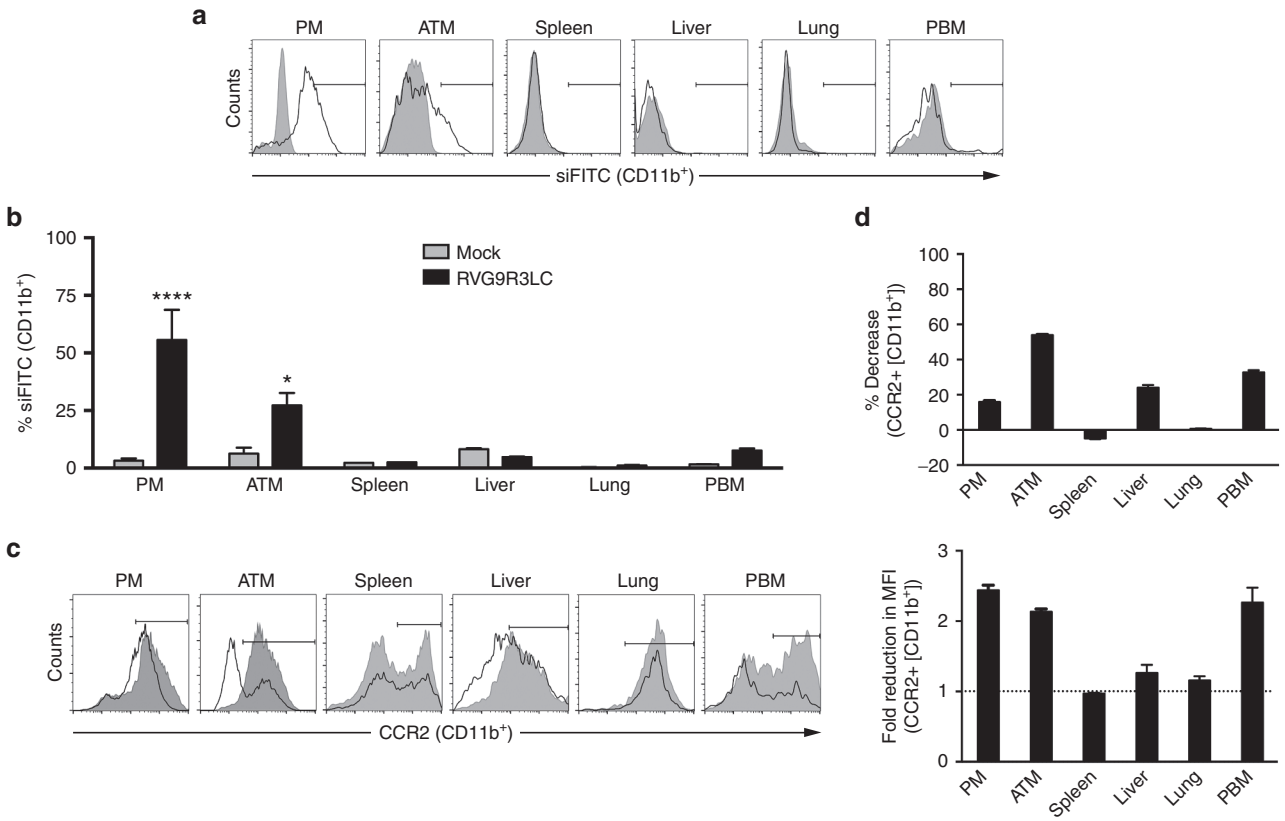

Figure 3 Intraperitoneal administration of RVG9R3LC targets siRNA into ATMs. (**a**,**b**) Flow cytometric analysis for fluorescent siRNA (siFITC) in CD11b$^+$ cells in the indicated tissues of high-fat diet (HFD)-fed mice after a single i.p. injection of RVG9R3LC:siRNA (400 pmol siRNA, 40:1 peptide:siRNA ratio). Representative histograms are shown in (**a**), and cumulative data in (**b**) depicting transfection efficiencies as percent CD11b$^+$ cells positive for FITC fluorescence. In (**a**), filled histograms represent mock-treated mice and the solid histograms represent cells isolated at 24 hours from mice treated with RVG9R3LC:siFITC. In (**b**), cells were scored as positive for uptake using the marker gate (black line) depicted in (a). (**c**,**d**) Flow cytometric analysis for CCR2 expression on CD11b$^+$ cells isolated from tissues of HFD-fed mice after i.p. injection of RVG9R3LC:siCCR2 (400 pmol siRNA, 40:1 peptide:siRNA ratio) for 3 weeks on alternate days. Representative histograms are shown in (**c**) with filled and solid histograms representing mice that were mock-treated or treated with RVG9R3L:siCCr2 complexes. Cumulative data in (**d**) depict CCR2 knockdown efficiencies as percent decrease in CCR2$^+$ CD11b$^+$ cells (left) and fold reduction in mean fluorescence intensity for CCR2 signal (right) in comparison to mock-treated mice. In (**d**), cells were scored as positive for CCR2 expression using the marker gate (black line) depicted in (**c**). The dashed line in the left panel depicts the value expected when there is no change in CCR2 expression. In all cases, error bars indicate SEM, $n = 3$–6. Significance was computed by analysis of variance and Bonferroni posttest in comparison to the values in mock-treated mice for each data set; $^*P < 0.05$, $^{****}P < 0.0001$. Mock, mice treated with naked siFITC or siCCR2; ATM, adipose tissue macrophages; PBM, peripheral blood macrophages; PM, peritoneal macrophages.

RVG9R3LC:siCCR2 treatment prevents macrophage infiltration into and inflammation in AT in obese mice

Infiltrating macrophages are a major cause for the inflammatory environment within AT in obese mice leading to metabolic dysfunction.[8–10] We assessed if CCR2 knockdown could disrupt macrophage chemotaxis into the AT in obese mice. HFD-fed C57BL/6 mice, with average body weights of 50 g, were treated i.p. with RVG9R3LC:siRNA complexes, three times a week for up to 6 weeks. Histological analysis of the eWAT showed a significant decrease in the numbers of "crown-like structures" that are formed by macrophages infiltrating the AT in RVG9R3LC:siCCR2 treated mice (**Figure 5a**). Although the overall mass of the AT was comparable in all mouse cohorts (not shown), the average numbers of crown-like structures per field in RVG9R3LC:siCCR2 treated mice were reduced by ~80% (**Figure 5b**). Accordingly, mRNA levels for CD11c and F4/80, the markers for M1 polarized macrophages,[15,21] were reduced by half as were levels of CD68 mRNA, indicating a lower number of total macrophages in eWAT in RVG9R3LC:siCCR2 treated mice (**Figure 5c**). mRNA levels for CD206, the marker for M2 macrophages, did not significantly change indicating that RVG9R3LC:siCCR2 treatment primarily contributes to reducing M1 macrophage infiltration and accumulation in the eWAT.

The outcome of decreased M1 macrophage frequencies on the inflammatory environment in the eWAT was reflected in significantly lower mRNA levels of TNF-α and inducible nitric oxide synthase, key inflammatory mediators in obesity[13–15] (**Figure 5d**). Consequently, serum concentrations of MCP-1 and IL-6, whose production is triggered by TNF-α, were ~50% lower in treated mice than in the control obese mouse groups (**Figure 5e**). Our data thus bolsters other studies demonstrating a reduction in M1-type macrophages correlates with a decrease in proinflammatory chemoattractant cytokines as well as circulating inflammatory cytokines.[42,48,49] Our data also demonstrate that downregulating CCR2 expression in

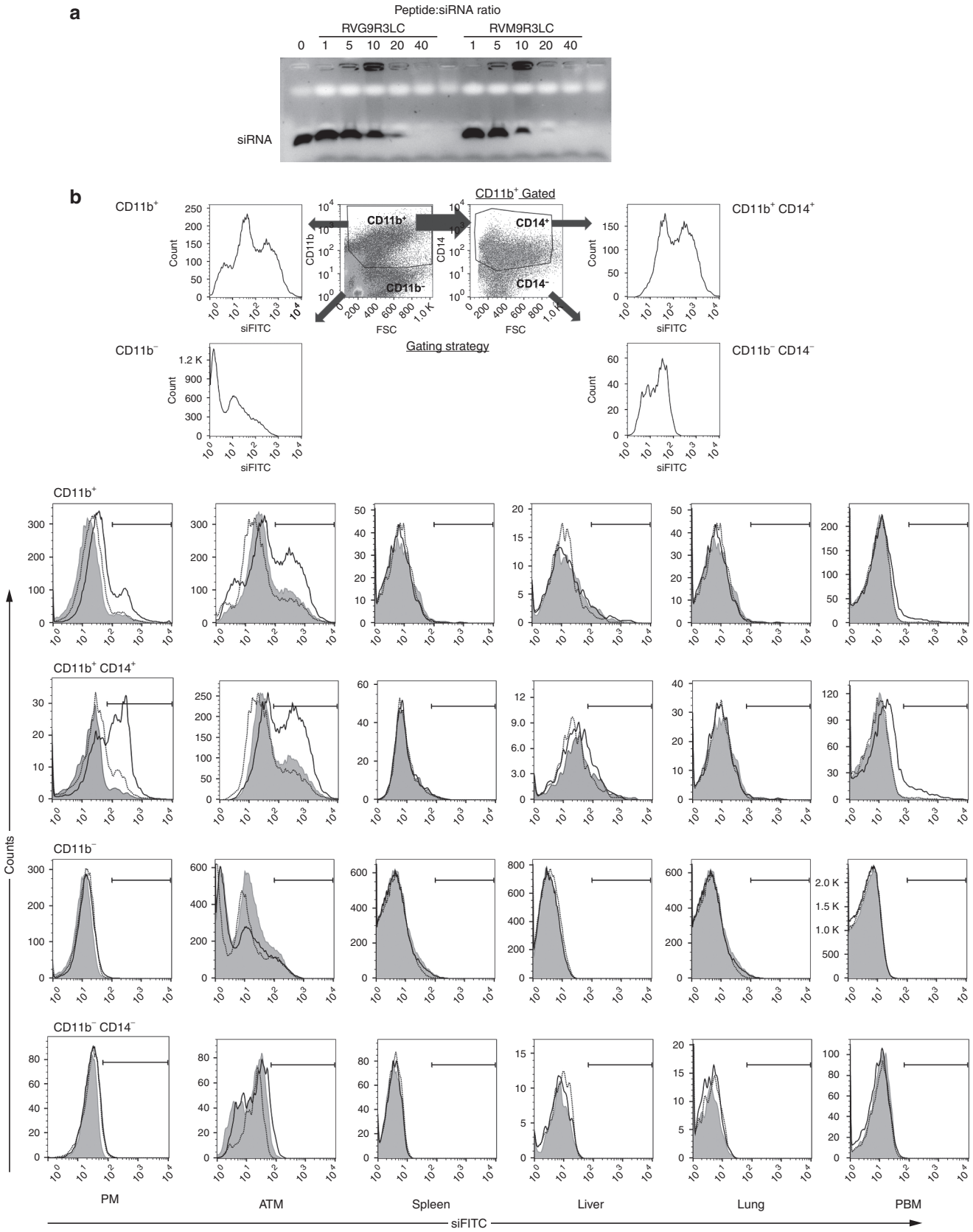
a
Peptide:siRNA ratio
RVG9R3LC
RVM9R3LC
0 1 5 10 20 40
1 5 10 20 40
siRNA
b
CD11b+
CD11b+ Gated
CD11b+ CD14+
CD11b−
CD11b− CD14−
Gating strategy
Count
siFITC
CD11b
FSC
CD14
Counts
PM
ATM
Spleen
Liver
Lung
PBM

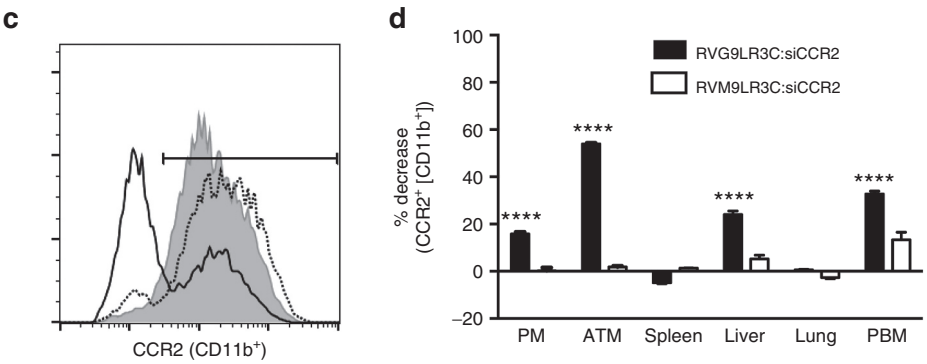

Figure 4 A nontargeting peptide cannot mediate functional siRNA delivery to macrophages. (**a**) Electrophoretic gel mobility shift assays with 100 pmol siRNA complexed to peptides RVG9R3LC and RVM9R3LC at the indicated molar excesses of the peptides. (**b**) A representation of the flow cytometric analysis for quantifying fluorescent siRNA (siFITC) in cells isolated from the indicated tissues of high-fat diet (HFD)-fed mice after a single i.p. injection of peptide:siRNA (400 pmol siRNA, 40:1 peptide:siRNA ratio). The gating strategy used to identify $CD11b^+$/$CD14^+$ is shown in the upper panel. The filled histograms represent mock-treated mice and the dotted and solid histograms represent cells isolated at 24 hours from mice treated with RVM9R3LC:siFITC and RVG9R3LC:siFITC. Cells were scored as positive for uptake using the marker gate (black line) depicted. (**c**) A representative flow cytometric histogram plot for CCR2 expression in $CD11b^+$ ATMs isolated from HFD-fed mice after i.p. injection of peptide:siCCR2 (400 pmol siRNA, 40:1 peptide:siRNA ratio) for 3 weeks on alternate days. The filled histograms represent mock-treated mice and the solid and dotted histograms represent mice treated with RVG9R3LC:siRNA and RVM9R3L:siRNA complexes, respectively. Cumulative data in (**d**) depict CCR2 knockdown efficiencies as percent decrease in $CCR2^+$ $CD11b^+$ cells in comparison to mock-treated mice. Significance was computed by multiple nonparametric *t*-tests, $^{****}P < 0.0001$. In all cases, error bars indicate SEM. Mock, mice treated with siRNA alone; ATM, adipose tissue macrophages; PBM, peripheral blood macrophages; PM, peritoneal macrophages.

macrophages by RVG9R3LC-delivered siRNA contributes to this effect by reducing M1 macrophage levels in the AT.

RVG9R3LC:siCCR2 treatment improves glucose tolerance and restores insulin sensitivity

To test the effects of reduced inflammation in the eWAT on whole-body metabolism, we measured responses to glucose and insulin challenges in HFD-fed mice (**Figure 6a–d**). RVG9R3LC:siCCR2 treatment improved glucose tolerance in obese mice (**Figure 6a**). Glucose tolerance test area under the curve calculations revealed that mice treated with RVG9R3LC:siCCR2 were significantly more tolerant to a glucose challenge when compared with mock- or control siRNA-treated mice (**Figure 6b**). To study the effects on systemic insulin sensitivity, we performed insulin tolerance tests (**Figure 6c,d**). Mice treated with RVG9R3LC:siCCR2, again, had a significant improvement in insulin response compared with mice in the two control groups. While no significant changes in food intake were recorded during the treatment period (**Supplementary Figure S2**), body weight gain was more gradual in RVG9R3LC:siCCR2-treated mice in contrast to mice in the control groups, which showed a steady and significant increase in body weight (**Figure 6e**). Taken together, these results suggest that RVG9R3LC:siCCR2 treatment for decreasing inflammatory macrophage chemotaxis into the AT also has a beneficial effect on whole-body metabolism.

RVG9R3LC:siCCR2 treatment ameliorates hepatic steatosis in obese mice

Hepatic steatosis, a consequence of obesity-induced inflammation, is a condition characterized by MCP-1/CCR2-induced myeloid cell recruitment into the liver.[25,26] Our observations indicated that RVG9R3LC:siCCR2 treatment reduced levels of $CCR2^+$ macrophages in the liver of HFD-maintained obese mice (**Figure 3c**,d). Therefore, we tested effects on hepatic steatosis. First, a comparison of the sizes and weights of livers indicated that RVG9R3LC:siCCR2 treatment reduced the mass of the hepatic organ in obese mice by >50%, indicating a significant decrease in hepatomegaly (**Figure 7a,b**). Next, histological analysis of liver tissue sections in obese mice revealed that the severe steatosis (both microvacuolar and macrovacuolar) was near completely reversed upon treatment with RVG9R3LC:siCCR2 (**Figure 7c**). The number of large-droplet liver cells in RVG9R3LC:siCCR2-treated mice were reduced (**Figure 7c**) and accordingly, an ~40% decrease in hepatic triglyceride (TG) content was recorded with respect to the control groups (**Figure 7d**). Corroborating this, mRNA levels of the lipogenic gene for TG synthesis, stearoyl-CoA desaturase 1 (SCD1), were also reduced by ~70%, indicating a likely reduction in circulating free fatty acid levels as this regulates *Scd1* expression.[50,51] Finally, we also detected ~70% reduction in tissue mRNA levels of TNF-α whose increased expression in the liver is associated with hepatic steatosis[25,52] (**Figure 7e**). These observations indicate that ATM-directed delivery of RVG9R3LC:siCCR2 protects against HFD-induced hepatic steatosis.

In conclusion, i.p. administration of the macrophage-binding RVG9R3LC peptide in obese mice enables targeting of inflamed peritoneal and ATMs. Exploiting this delivery system to disrupt macrophage chemotaxis to the AT and liver, through siRNA-mediated downregulation of CCR2, holds immense utility in treating the complications associated with diet-induced obesity.

Discussion

The highlight of this study is a strategy for treating obesity-induced inflammation through silencing of genes in macrophages that contribute to this condition. A distinct biodistribution profile with selective targeting of peritoneal and

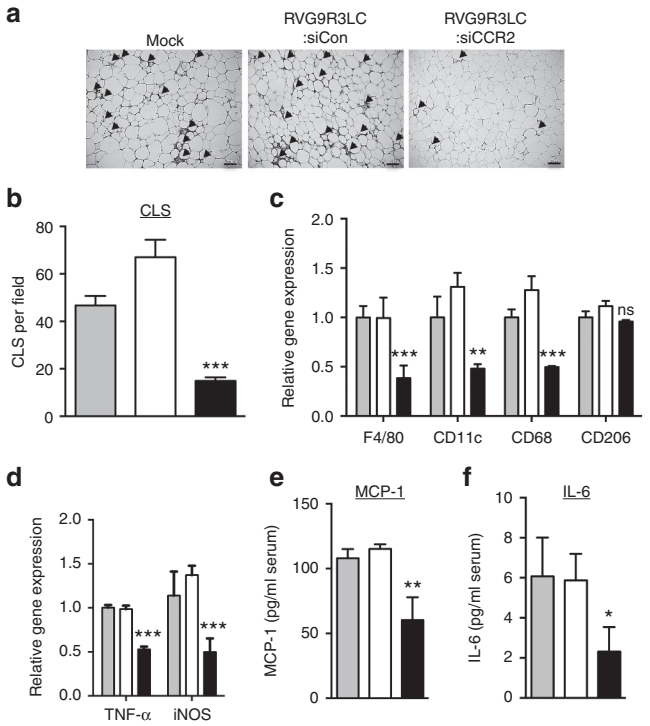

Figure 5 Treatment of diet-induced obese mice with RVG9R3LC:siCCR2 reduces macrophage infiltration and inflammatory chemokine production in adipose tissues. Mice maintained on high-fat diet (HFD) were treated i.p. with RVG9R3LC:siRNA complexes (400 pmol siRNA) as indicated on alternate days for 6 weeks (**a**) Representative H&E-stained sections of epididymal white adipose tissue (eWAT) with arrowheads indicating CLS or areas of macrophage infiltration around adipocytes. Scale bar = 100 μm. Scale bar = 100 μm. (**b**) Quantification of CLS and (**c**) quantitative PCR (qPCR) quantitation of M1 macrophage-specific mRNA F4/80, CD68, CD11c, and M2 mRNA macrophage-specific CD206 in eWAT. 36B4 mRNA was used for normalizing. (**d**) qPCR quantitation of mRNAs for the proinflammatory cytokine TNF-α and iNOS in eWAT. mGAPDH was used for normalizing. In (**c**) and (**d**), data are presented relative to the corresponding mRNA expression level in HFD-fed obese mice. Serum MCP-1 (**e**) and IL-6 (**f**) levels determined by ELISA. In all cases, the grey, white, and black bars represent mock-, control RVG9R3LC:siCD4-, and RVG9R3LC:siCCR2-treated mice, respectively. Error bars indicate SEM. Significance was computed by analysis of variance and Bonferroni posttest in comparison to the values in mock-treated mice for each data set; $^{*}P < 0.05$, $^{**}P < 0.01$, $^{***}P < 0.001$. ns, nonsignificant. Each group of mice comprised three to six animals. Mock, mice treated with naked siCCR2; siCon, siRNA targeting human CD4; CLS, crown-like structures; IL, interleukin; iNOS, inducible nitric oxide synthase; MCP-1, monocyte chemoattractant protein-1; TNF, tumor necrosis factor.

AT macrophages was achieved using a macrophage-binding peptide and an i.p. route of administration. Delivery of siRNA for silencing the expression of CCR2, a gene product that mediates migration of macrophages to the visceral AT in obese rodents and humans,[8–10] using this strategy provided therapeutic benefits in obese mice.

In this study of macrophage-targeted RNAi in diet-induced obesity mice, we corroborate and extend evidence for the role of the CCR2/MCP-1 signaling pathway in the inflammation that drives insulin resistance and hyperglycemia in dietary obese mice. We used a rabies virus-derived peptide that binds nAchR subunits, and which in previous studies, was shown to be to target peripheral blood macrophages and microglia upon intravenous injection in mice.[37,39,40,53] An i.p. route of administration, in contrast, elicited siRNA delivery into macrophages in the peritoneum and the inflamed AT in HFD-fed mice. Previous studies demonstrate glucan shells (glucan-encapsulated siRNA particles) and gold nanoparticles selectively localized to the AT (and not other tissues/organs) only through an i.p. injection route.[42,43] Further, basic drugs and cationic peptides/protein conjugates also have a propensity to infiltrate the AT.[44–46] We hypothesize that the i.p. route of injection together with the highly basic 9R cell-penetrating peptide contribute to AT infiltration and macrophage targeting by the nAchR-binding RVG9R3LC peptide:siRNA nanoparticles. It is also possible that macrophages in the peritoneum bind the nanoparticles and then traffic to the AT enhancing AT delivery.

i.p. treatment with the RVG9R3LC peptide complexed to anti-CCR2 siRNA enabled (i) reduction of CCR2 expression on macrophages, (ii) reduced macrophage infiltration into and therefore decreased M1 macrophage levels within the eWAT, and (iii) reduced tissue and serum levels of inflammatory cytokines secreted monocytes and macrophages that are strongly associated with metabolic dysregulation during obesity (for a review, see ref. 54). For instance, TNF-α can reduce tyrosine phosphorylation of the insulin receptor substrate-1 (IRS-1) and downregulate adipogenic genes such as PPAR-γ and C/EBP, leading to impaired insulin action.[55–57] Further, via the activation of MAPK and NF-κB signaling pathways, TNF-α augments the release of IL-1β and IL-6[58,59], that inhibit insulin-stimulated glucose uptake and serine phosphorylation of IRS-1, respectively.[60–62] Additionally elevated WAT-derived TNF-α secretion is one of many factors implicated in hepatic insulin resistance.[63] Hepatic insulin resistance can enhance *de novo* lipogenesis leading to chronic hyperglycemia and hypertriglyceridemia, which are among the collection of pathogenic states that represent hepatic steatosis.[64,65] Consequently, reducing inflammatory cytokine production by inhibiting macrophage migration into the WAT allowed significant improvements in glucose metabolism, insulin sensitivity, and mitigation of pathogenic parameters that represent HFD-induced hepatic steatosis.

There is no doubt that weight loss can improve the inflammatory phenotype in obese conditions,[66] however rapid and sustained weight loss is rarely possible. There has thus been a push towards identifying alternative interventions that may antagonize inflammation independent of weight loss (reviewed in ref. 54). Mice genetically knocked out for genes that play a role in obesity-induced inflammation, including MCP-1, have improved glucose homeostasis and reduced liver fat content and liver mass compared to wild-type mice maintained on HFD despite similar body weights.[25,67] Treatment of diabetic db/db mice with a CCR2 antagonist for 12 weeks in addition to reversing insulin resistance also improved lipid metabolism and reduced liver fat content without influencing body mass.[68] In our studies, a small but significant reduction in body weight occurring towards the end of the observation period (week 7), which might have translated to increased weight loss, had the treatment been prolonged.

As CCR2-expressing cells are recruited through interactions with MCP-1 as well as with other cytokines produced by the inflamed AT,[7,25,33] interfering with CCR2 expression or

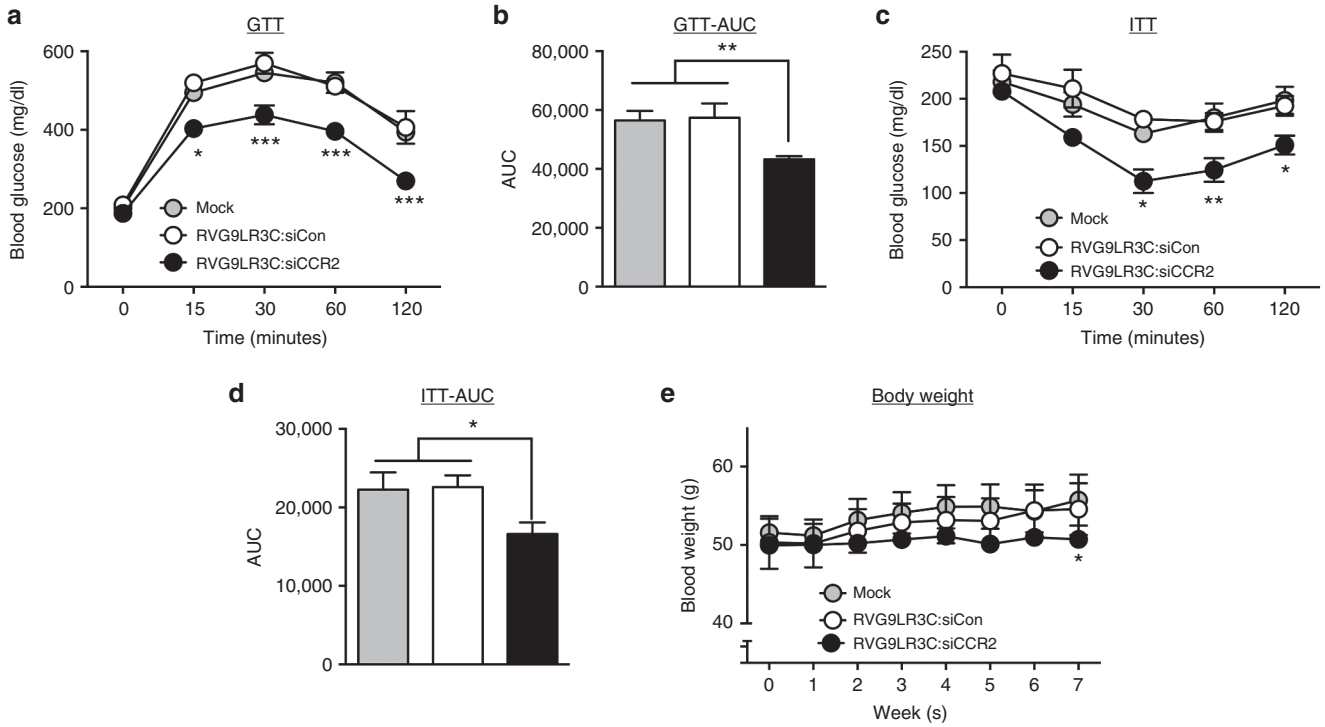

Figure 6 RVG9R3LC/siCCR2 treatment reverses glucose intolerance and insulin resistance. Serum glucose levels in high-fat diet (HFD)-fed obese mice upon (**a**) a GTT and (**c**) an ITT after a 12 and 4 hours fasting period at the indicated time points. (**b,d**) AUC of corresponding GTT (a) and ITT (**c**) graphs. Data presented relative to AUC values in untreated HFD-fed obese mice. Wherever relevant, the grey, white, and black bars represent mock-, control RVG9R3LC-siCD4-, and RVG9R3LC-siCCR2-treated mice, respectively. Error bars indicate SEM, $n = 3$. Statistical significance was determined by analysis of variance and the Tukey (**a** and **c**) or Bonferroni (**b**, **d**, and **e**) posttests in comparison to the values in mock-treated mice for each data set; $^{*}P < 0.05$, $^{**}P < 0.01$, $^{***}P < 0.001$. Mock, mice treated with naked siCCR2; siCon, siRNA targeting human CD4; AUC, area under the curve; GTT, glucose tolerance tests; ITT, insulin tolerance tests.

function may be more advantageous than blocking MCP-1. A number of small-molecule antagonists of CCR2 exist (reviewed in refs. 69,70) but only few have been tested for activity against obesity-induced inflammation *in vivo*.[29,52,68,71–73] A phase 2 clinical trial has indicated beneficial effects of the CCR2 antagonist CCX140-B on glycemic parameters in human subjects.[71] It is, however, well acknowledged that suboptimal pharmacokinetics/pharmacodynamics, low AT penetrance, and toxicity are significant problems associated with the use of pharmacological inhibitors as intervention for AT inflammation.[52,70,72,74,75] Furthermore, the important immunomodulatory and protective effects of CCR2 activity,[76–78] particularly in resolving pathology during viral infections,[79,80] advocates restricting CCR2 blockade to tissues/organs of pharmacological interest.

The relative paucity of *in vivo* delivery systems for macrophages has impeded the use of siRNA-based approaches as treatment for macrophage-associated inflammation during diet-induced obesity. In a proof-of-concept study, JNK1 knockdown in HFD-fed mice as well as genetically obese mice using shRNA-expressing adenoviral vectors decreased plasma glucose levels and steatosis, but the site of action was localized to the hepatic tissue given that route of administration was intravenous and the liver is the target organ for systemically administered nanoparticles and viral vectors.[81] Another study with a systemically administered lipid nanoparticle formulation resulted in the accumulation of anti-CCR2 siRNA in multiple lineages of immune cells in the spleen, blood, and bone marrow and promoted islet graft survival in type 1 diabetic mice by preventing mobilization of monocytes to the grafted tissue.[82] Glucan-based shells, incorporating *Saccharomyces cerevisiae* β-1,3-D-glucan, ligand that binds the dectin-1 receptor expressed on macrophages, have been successful in eliciting siRNA delivery to phagocytic macrophages *in vivo*.[83,84] Interestingly, i.p. administration of siRNA encapsulated within glucan shells selectively targeted visceral ATMs in obese mice, and not macrophages in other tissues.[42] Silencing TNF-α or osteopontin gene expression in visceral ATMs using this strategy improved glucose tolerance in obese mice but did not impact circulating TGs or hepatic steatosis due to the restricted biodistribution of this formulation.

It is our view that disrupting macrophage chemotaxis to inflamed tissues during diet-induced obesity is more effective as treatment than blockade of proinflammatory effector cytokines as this can also minimize the profound paracrine and endocrine effects exerted by the recruited cells. Indeed, although RVG9R3L-mediated siRNA delivery occurred primarily to peritoneal macrophages and ATMs, an additional consequence of treating with siRNA targeting CCR2 was a pronounced reduction in CCR2-expressing hepatic $CD11b^{+}$ macrophages, signifying inhibition of macrophage trafficking to the liver. A second reason contributing to this outcome could be an altered peptide-siRNA distribution profile

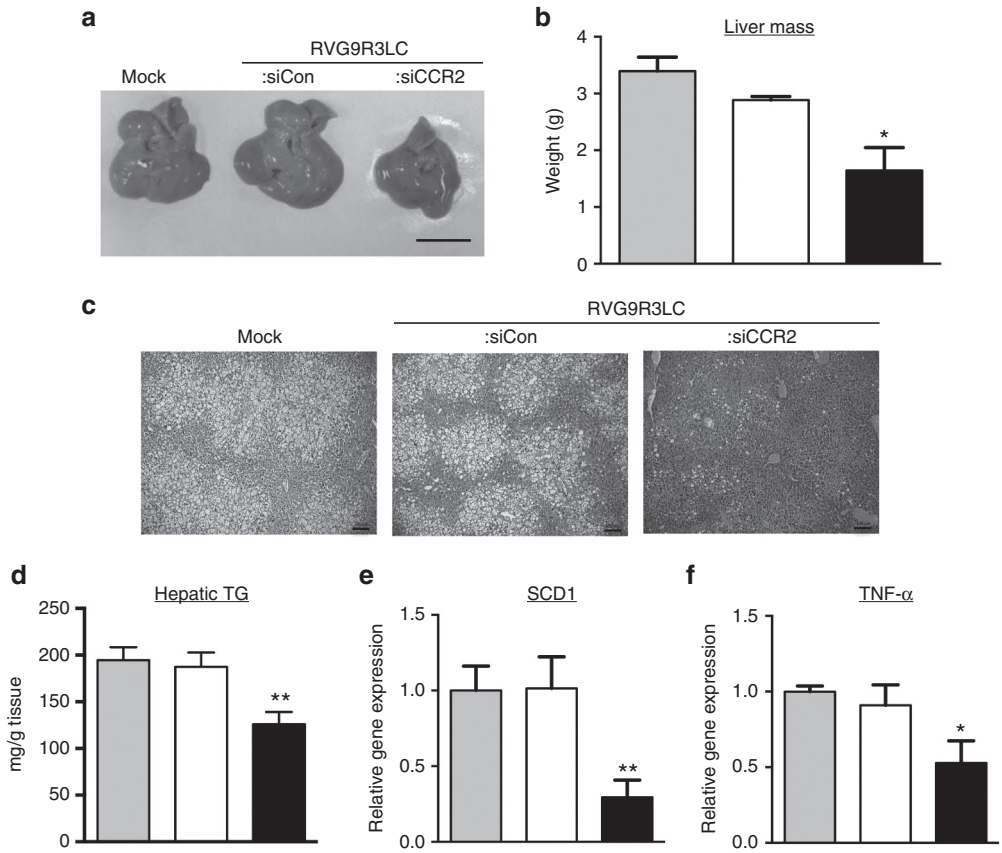

Figure 7 RVG9R3LC/siCCR2 treatment ameliorates hepatic steatosis and inflammation in dietary obese mice. Representative images of liver (**a**) and average organ weight (**b**) from obese mice treated as indicated; scale bar = 100 µm. (**c**) Representative H&E stained sections of liver tissue. Scale bar = 100 µm. (**d**) hepatic TG content, (**e**), and (**f**) quantitative PCR quantitation of SCD1 and TNF-α mRNA with mGAPDH mRNA levels used for normalization. Data are presented relative mRNA levels in untreated high-fat diet-fed obese mice. In all cases, the grey, white, and black bars represent mock-, control RVG9R3LC-siCD4- and RVG9R3LC-siCCR2-treated mice, respectively. Error bars indicate SEM, $n = 3$ or 4. Significance was computed by analysis of variance and Bonferroni posttest in comparison to the values in mock-treated mice for each data set; $^{*}P < 0.05$, $^{**}P < 0.01$. Mock, mice treated with naked siCCR2; siCon, siRNA targeting human CD4; SCD1, stearoyl-CoA desaturase 1; TG, triglyceride; TNF, tumor necrosis factor.

that includes the hepatic tissue upon prolonged administration. The mechanism of siRNA delivery, which is transport across the plasma membrane and into the cytoplasm after RVG9LR3C binds receptors on macrophages[38] and not phagocytosis like in the case of glucan shells, would then contribute towards a functional outcome in tissue-resident macrophages.

The targeted delivery approach also conferred the huge advantage of reduced dosing an improved outcome attained after 6 weeks of treatment with as little as 0.1 mg/kg body weight of siRNA administered three times a week. Our previous studies have indicated minimal immunogenicity of nonadjuvanted RVG peptides after repeated systemic administration in mice.[37] The very easy formulation protocol, which involves simple mixing of the peptide with siRNAs to form complexes within a matter of minutes, makes RVG9LR3C a versatile siRNA delivery platform that may be used for the combinatorial targeting of more than one gene product that regulate the inflammatory pathway in macrophages to achieve higher therapeutic potency.

In conclusion, in animal models of diet-induced obesity, silencing of CCR2 in macrophages can reduce inflammation in AT, ameliorate multiple diabetic parameters, and restore hepatic metabolism. Thus, CCR2 siRNA might provide a treatment strategy for human obesity-associated inflammation, and RVG9R3LC, a tool to deliver siRNA to macrophages for suppressing a variety of therapeutic targets in human inflammatory diseases.

Materials and methods

Peptide and siRNAs. RVG9R3LC and RVM9R3LC were synthesized by Peptron (Daejeon, Korea). siRNAs siCCR2 (5′-GCUAAACGUCUCUGCAAAdTdT-3′)[82] and siCD4[85] were synthesized by ST Pharm (Seoul, Korea). FITC-labeled siRNA referred to as siFITC targets the firefly luciferase mRNA.[39]

Electrophoretic mobility shift assay. About 100 pmol siRNA was preincubated with RVG9R3LC at the indicated peptide:siRNA molar ratios for 30 minutes at room temperature. The samples were loaded onto a 1% agarose gel and electrophoresed. Ethidium bromide was used for visualization of the siRNA bands.

Physical characterization of RVG9R3LC:siRNA complexes. About 100 pmol siRNA was suspended in 100 µl of distilled water with RVG9R3LC at the indicated peptide:siRNA molar ratios. After incubation for 30 minutes, the average particle size and zeta potential were measured by using dynamic light scattering (Zetasizer-nano analyzer Zs; Malvern Instruments, Worcestershire, UK). Mean values were obtained from three runs at 25 °C.

Cell culture. The murine monocyte cell line Raw 264.7 was obtained from ATCC and cultured in Dulbecco's modified Eagle's medium containing 10% fetal bovine serum and penicillin–streptomycin (100 IU/ml). Peritoneal macrophages were harvested from C57BL/6 mice as previously reported[86] and seeded at 1×10^6 cells/ml in RPMI 1640 supplemented with 10% fetal bovine serum and 1% antibiotics for further experiments.

Cytotoxicity assay. Cytotoxicity was assessed using the CCK-8 assay (Dojindo Laboratories, Kumamoto, Japan) at 24 hours posttransfection followed by manufacturer's instruction.

In vitro siRNA transfection experiments. About 100 pmol FITC-labeled siRNA (siFITC), siCD4, or siCCR2 were complexed with RVG9R3LC (1:10–80 siRNA:peptide molar ratios) and added to 2×10^5 cells (Raw 264.7 cells or peritoneal macrophages) cultured per well of a 12-well plate. Transfections with Lipofectamine 2000 (Invitrogen, Seoul Korea) were performed according to the manufacturer's instructions. Twenty-four hours later, cellular uptake of siFITC was quantified using flow cytometry and siRNA functionality analyzed by quantitative PCR for CCR2 mRNA. mRNA levels were normalized to that of murine GAPDH mRNA levels. The primers used in the experiments are presented in **Supplementary Table 1**.

In vivo siRNA transfer experiments. Male C57BL/6 mice (6 weeks old, 20–22 g of body weight) were purchased from Orient Bio (Seoul, Korea). Mice were fed normal chow (13.5% fat; LabDiet) or a HFD (60% fat; Research Diets) for 12 weeks to establish obese conditions wherein the average body weight exceeded 50 g. Animals were housed in a pathogen-free facility and given free access to food and water. All experimental procedures were approved by the Institutional Animal Care and Use Committee of Hanyang University. Each experiment was conducted with mouse cohorts of at least four mice per experimental group.

To evaluate RVG9R3LC-mediated siRNA delivery, 400 pmol of siFITC was complexed with RVG9R3LC and RVM-9R3LC (40:1 peptide:siRNA molar ratio) in 200 µl of Dulbecco's phosphate-buffered saline (pH 7.4). After a 30-minute incubation, the peptide:siRNA complex was i.p. injected into HFD-fed obese mice that were at least 50 g in body weight. Twenty-four hours later, eWAT, spleen, lung, and liver tissues were isolated, washed in cold phosphate-buffered saline, and minced before enzymatic digestion with collagenase (2 mg/ml) for 1 hour at 37 °C. Single-cell suspensions obtained by passing through 100-µm cell strainers were treated with red blood cell lysis buffer (Life Technologies) to remove red blood cells. These cells were stained alongside mononuclear cells isolated from the peritoneal cavity by washing with phosphate-buffered saline and Ficoll purification of peripheral blood. Antibodies to murine CD11b and CD14 (PE- or APC-labeled) were used for staining prior to flow cytometric analysis. To assess functionality of siRNA delivered, siCCR2 was complexed with RVG9R3LC or RVM9R3LC (40:1 molar ratio, 0.1 mg siRNA/kg body weight) using the same conditions as above, and the complexes were injected every alternate day for a period of 3 weeks. Subsequently, cells were isolated and costained with CD11b-PE and CCR2-APC antibodies (R&D Systems) and analyzed by flow cytometry.

To evaluate the effects of CCR2 knockdown *in vivo*, mice maintained on HFD were injected i.p. with RVG9R3LC:siRNA complexes generated as above (400 pmol siRNA, 40:1 peptide:siRNA ratio) in 200 µl of Dulbecco's phosphate-buffered saline (pH 7.4) on alternate days for a period of 6 weeks. Caloric intake was not measured; however, food intake was comparable in all groups. Body weights of mice were measured every week after the first treatment. After siRNA treatment, metabolic tests performed as described below. AT and liver were harvested from euthanized mice, weighed, and snap-frozen in liquid nitrogen for further analysis. Blood was also collected to obtain serum for ELISA tests.

Cytokine ELISA and measurements of hepatic TG content. Serum cytokine levels were measured using ELISA kits for the detection of MCP-1 and IL-6 (eBioscience San Diego, CA), and hepatic TG content was determined using the Triglyceride Colorimetric Assay Kit (Cayman, Ann Arbor, MI). All analyses were conducted in triplicate.

Metabolic studies. Glucose tolerance tests and insulin tolerance tests were performed a week before sacrifice as previously described.[87] Briefly, for glucose tolerance test, mice were fasted overnight, followed by i.p. injection with glucose (1 g/kg body weight). For insulin tolerance test, mice were fasted for 4 hours before i.p. injecting human insulin (0.75 units/kg). Blood samples were collected from the tail vein at 0, 15, 30, 60, and 120 minutes after administration of glucose or insulin and blood sugar levels measured by ACCU-CHECK (Roche, Carlsbad, CA) as per the manufacturers' protocols.

Gene expression analysis. Total mRNA was extracted from the eWAT or livers of mice using the RNAiso kit (Takara). cDNA was prepared by the use of iScript TM cDNA synthesis kit (Bio-Rad Laboratories) with 1 µg of mRNA. The quantitative evaluation of mRNA was carried out with a 7500 Real-Time PCR system (Applied Biosystems) using SYBR premix ExTaq perfect real time (Takara, Shiga, Japan). Values were normalized to mGAPDH mRNA levels. The primers used in the experiments are described in **Supplementary Table 1**.

Histology. Tissue samples from eWAT or livers were fixed in 4% paraformaldehyde in Dulbecco's phosphate-buffered saline, followed by embedding in paraffin blocks prior to sectioning. The sections were stained with hematoxylin and eosin (H&E).

Statistical analysis. Data are presented as mean ± SEM or mean ± SD as indicated. Statistical significance was analyzed using analysis of variance (one-way or two-way, multiple comparison) with Bonferroni post test. $P < 0.05$ was considered significant.

Supplementary material

Table S1. Primer sequences used in this study
Figure S1. Evaluation of toxicity.
Figure S2. Daily food intake in the mouse cohorts.

Acknowledgments This work was partially supported by NIH, grant R01AI112443 to P.K. and the Korea National Research Foundation (2014R1A1A2056664) to S.-K.L. S.-K.L. is a Yang Young Foundation Scholar. J.K., K.C., C.C., J.B., I.U., and N.K. performed the research; K.Y.L., S.-K.L., and P.K. designed the experiments and/or analyzed the data; J.K., S.-K.L., and P.K. wrote the manuscript. The authors declare no competing financial interests.

1. Chawla, A, Nguyen, KD and Goh, YP (2011). Macrophage-mediated inflammation in metabolic disease. *Nat Rev Immunol* **11**: 738–749.
2. Gregor, MF and Hotamisligil, GS (2011). Inflammatory mechanisms in obesity. *Annu Rev Immunol* **29**: 415–445.
3. Hossain, P, Kawar, B and El Nahas, M (2007). Obesity and diabetes in the developing world–a growing challenge. *N Engl J Med* **356**: 213–215.
4. Hotamisligil, GS (2006). Inflammation and metabolic disorders. *Nature* **444**: 860–867.
5. Kahn, SE, Hull, RL and Utzschneider, KM (2006). Mechanisms linking obesity to insulin resistance and type 2 diabetes. *Nature* **444**: 840–846.
6. Donath, MY and Shoelson, SE (2011). Type 2 diabetes as an inflammatory disease. *Nat Rev Immunol* **11**: 98–107.
7. Ota, T (2013). Chemokine systems link obesity to insulin resistance. *Diabetes Metab J* **37**: 165–172.
8. Cancello, R, Henegar, C, Viguerie, N, Taleb, S, Poitou, C, Rouault, C *et al.* (2005). Reduction of macrophage infiltration and chemoattractant gene expression changes in white adipose tissue of morbidly obese subjects after surgery-induced weight loss. *Diabetes* **54**: 2277–2286.
9. Weisberg, SP, McCann, D, Desai, M, Rosenbaum, M, Leibel, RL and Ferrante, AW Jr. (2003). Obesity is associated with macrophage accumulation in adipose tissue. *J Clin Invest* **112**: 1796–1808.
10. McNelis, JC and Olefsky, JM (2014). Macrophages, immunity, and metabolic disease. *Immunity* **41**: 36–48.
11. Ahlin, S, Sjöholm, K, Jacobson, P, Andersson-Assarsson, JC, Walley, A, Tordjman, J *et al.* (2013). Macrophage gene expression in adipose tissue is associated with insulin sensitivity and serum lipid levels independent of obesity. *Obesity (Silver Spring)* **21**: E571–E576.
12. Hardy, OT, Perugini, RA, Nicoloro, SM, Gallagher-Dorval, K, Puri, V, Straubhaar, J *et al.* (2011). Body mass index-independent inflammation in omental adipose tissue associated with insulin resistance in morbid obesity. *Surg Obes Relat Dis* **7**: 60–67.
13. Baker, RG, Hayden, MS and Ghosh, S (2011). NF-κB, inflammation, and metabolic disease. *Cell Metab* **13**: 11–22.
14. Dallaire, P, Bellmann, K, Laplante, M, Gélinas, S, Centeno-Baez, C, Penfornis, P *et al.* (2008). Obese mice lacking inducible nitric oxide synthase are sensitized to the metabolic actions of peroxisome proliferator-activated receptor-gamma agonism. *Diabetes* **57**: 1999–2011.
15. Lumeng, CN, Bodzin, JL and Saltiel, AR (2007). Obesity induces a phenotypic switch in adipose tissue macrophage polarization. *J Clin Invest* **117**: 175–184.
16. Lumeng, CN and Saltiel, AR (2011). Inflammatory links between obesity and metabolic disease. *J Clin Invest* **121**: 2111–2117.
17. Guilherme, A, Virbasius, JV, Puri, V and Czech, MP (2008). Adipocyte dysfunctions linking obesity to insulin resistance and type 2 diabetes. *Nat Rev Mol Cell Biol* **9**: 367–377.
18. Samuel, VT, Petersen, KF and Shulman, GI (2010). Lipid-induced insulin resistance: unravelling the mechanism. *Lancet* **375**: 2267–2277.
19. Mantovani, A, Sica, A, Sozzani, S, Allavena, P, Vecchi, A and Locati, M (2004). The chemokine system in diverse forms of macrophage activation and polarization. *Trends Immunol* **25**: 677–686.
20. Mosser, DM and Edwards, JP (2008). Exploring the full spectrum of macrophage activation. *Nat Rev Immunol* **8**: 958–969.
21. Fujisaka, S, Usui, I, Bukhari, A, Ikutani, M, Oya, T, Kanatani, Y *et al.* (2009). Regulatory mechanisms for adipose tissue M1 and M2 macrophages in diet-induced obese mice. *Diabetes* **58**: 2574–2582.
22. Romeo, GR, Lee, J and Shoelson, SE (2012). Metabolic syndrome, insulin resistance, and roles of inflammation–mechanisms and therapeutic targets. *Arterioscler Thromb Vasc Biol* **32**: 1771–1776.
23. Goran, MI and Alderete, TL (2012). Targeting adipose tissue inflammation to treat the underlying basis of the metabolic complications of obesity. *Nestle Nutr Inst Workshop Ser* **73**: 49–60; discussion p61.
24. Kamei, N, Tobe, K, Suzuki, R, Ohsugi, M, Watanabe, T, Kubota, N *et al.* (2006). Overexpression of monocyte chemoattractant protein-1 in adipose tissues causes macrophage recruitment and insulin resistance. *J Biol Chem* **281**: 26602–26614.
25. Kanda, H, Tateya, S, Tamori, Y, Kotani, K, Hiasa, K, Kitazawa, R *et al.* (2006). MCP-1 contributes to macrophage infiltration into adipose tissue, insulin resistance, and hepatic steatosis in obesity. *J Clin Invest* **116**: 1494–1505.
26. Obstfeld, AE, Sugaru, E, Thearle, M, Francisco, AM, Gayet, C, Ginsberg, HN *et al.* (2010). C-C chemokine receptor 2 (CCR2) regulates the hepatic recruitment of myeloid cells that promote obesity-induced hepatic steatosis. *Diabetes* **59**: 916–925.
27. Sartipy, P and Loskutoff, DJ (2003). Monocyte chemoattractant protein 1 in obesity and insulin resistance. *Proc Natl Acad Sci USA* **100**: 7265–7270.
28. Simeoni, E, Hoffmann, MM, Winkelmann, BR, Ruiz, J, Fleury, S, Boehm, BO *et al.* (2004). Association between the A-2518G polymorphism in the monocyte chemoattractant protein-1 gene and insulin resistance and Type 2 diabetes mellitus. *Diabetologia* **47**: 1574–1580.
29. Weisberg, SP, Hunter, D, Huber, R, Lemieux, J, Slaymaker, S, Vaddi, K *et al.* (2006). CCR2 modulates inflammatory and metabolic effects of high-fat feeding. *J Clin Invest* **116**: 115–124.
30. Bruun, JM, Lihn, AS, Pedersen, SB and Richelsen, B (2005). Monocyte chemoattractant protein-1 release is higher in visceral than subcutaneous human adipose tissue (AT): implication of macrophages resident in the AT. *J Clin Endocrinol Metab* **90**: 2282–2289.
31. Christiansen, T, Richelsen, B and Bruun, JM (2005). Monocyte chemoattractant protein-1 is produced in isolated adipocytes, associated with adiposity and reduced after weight loss in morbid obese subjects. *Int J Obes (Lond)* **29**: 146–150.
32. Pandzic Jaksic, V, Gizdic, B, Miletic, Z, Trutin-Ostovic, K and Jaksic, O (2013). Association of monocyte CCR2 expression with obesity and insulin resistance in postmenopausal women. *Clin Invest Med* **36**: E24–E31.
33. Ouchi, N, Parker, JL, Lugus, JJ and Walsh, K (2011). Adipokines in inflammation and metabolic disease. *Nat Rev Immunol* **11**: 85–97.
34. Kanasty, R, Dorkin, JR, Vegas, A and Anderson, D (2013). Delivery materials for siRNA therapeutics. *Nat Mater* **12**: 967–977.
35. Lorenzer, C, Dirin, M, Winkler, AM, Baumann, V and Winkler, J (2015). Going beyond the liver: progress and challenges of targeted delivery of siRNA therapeutics. *J Control Release* **203**: 1–15.
36. Kumar, P, Ban, HS, Kim, SS, Wu, H, Pearson, T, Greiner, DL *et al.* (2008). T cell-specific siRNA delivery suppresses HIV-1 infection in humanized mice. *Cell* **134**: 577–586.
37. Kumar, P, Wu, H, McBride, JL, Jung, KE, Kim, MH, Davidson, BL *et al.* (2007). Transvascular delivery of small interfering RNA to the central nervous system. *Nature* **448**: 39–43.
38. Zeller, S, Choi, CS, Uchil, PD, Ban, HS, Siefert, A, Fahmy, TM *et al.* (2015). Attachment of cell-binding ligands to arginine-rich cell-penetrating peptides enables cytosolic translocation of complexed siRNA. *Chem Biol* **22**: 50–62.
39. Kim, SS, Ye, C, Kumar, P, Chiu, I, Subramanya, S, Wu, H *et al.* (2010). Targeted delivery of siRNA to macrophages for anti-inflammatory treatment. *Mol Ther* **18**: 993–1001.
40. Subramanya, S, Kim, SS, Abraham, S, Yao, J, Kumar, M, Kumar, P *et al.* (2010). Targeted delivery of small interfering RNA to human dendritic cells to suppress dengue virus infection and associated proinflammatory cytokine production. *J Virol* **84**: 2490–2501.
41. Carralot, JP, Kim, TK, Lenseigne, B, Boese, AS, Sommer, P, Genovesio, A *et al.* (2009). Automated high-throughput siRNA transfection in raw 264.7 macrophages: a case study for optimization procedure. *J Biomol Screen* **14**: 151–160.
42. Aouadi, M, Tencerova, M, Vangala, P, Yawe, JC, Nicoloro, SM, Amano, SU *et al.* (2013). Gene silencing in adipose tissue macrophages regulates whole-body metabolism in obese mice. *Proc Natl Acad Sci USA* **110**: 8278–8283.
43. Chen, H, Dorrigan, A, Saad, S, Hare, DJ, Cortie, MB and Valenzuela, SM (2013). *In vivo* study of spherical gold nanoparticles: inflammatory effects and distribution in mice. *PLoS One* **8**: e58208.
44. Betschart, HR, Jondorf, WR and Bickel, MH (1988). Differences in adipose tissue distribution of basic lipophilic drugs between intraperitoneal and other routes of administration. *Xenobiotica* **18**: 113–121.
45. Wancewicz, EV, Maier, MA, Siwkowski, AM, Albertshofer, K, Winger, TM, Berdeja, A *et al.* (2010). Peptide nucleic acids conjugated to short basic peptides show improved pharmacokinetics and antisense activity in adipose tissue. *J Med Chem* **53**: 3919–3926.
46. Park, YS, David, AE, Huang, Y, Park, JB, He, H, Byun, Y *et al.* (2012). *In vivo* delivery of cell-permeable antisense hypoxia-inducible factor 1α oligonucleotide to adipose tissue reduces adiposity in obese mice. *J Control Release* **161**: 1–9.
47. Bu, L, Gao, M, Qu, S and Liu, D (2013). Intraperitoneal injection of clodronate liposomes eliminates visceral adipose macrophages and blocks high-fat diet-induced weight gain and development of insulin resistance. *AAPS J* **15**: 1001–1011.
48. Kobayashi, N, Ueki, K, Okazaki, Y, Iwane, A, Kubota, N, Ohsugi, M *et al.* (2011). Blockade of class IB phosphoinositide-3 kinase ameliorates obesity-induced inflammation and insulin resistance. *Proc Natl Acad Sci USA* **108**: 5753–5758.
49. Mothe-Satney, I, Filloux, C, Amghar, H, Pons, C, Bourlier, V, Galitzky, J *et al.* (2012). Adipocytes secrete leukotrienes: contribution to obesity-associated inflammation and insulin resistance in mice. *Diabetes* **61**: 2311–2319.

50. Li, ZZ, Berk, M, McIntyre, TM and Feldstein, AE (2009). Hepatic lipid partitioning and liver damage in nonalcoholic fatty liver disease: role of stearoyl-CoA desaturase. *J Biol Chem* **284**: 5637–5644.
51. Alkhouri, N, Dixon, LJ and Feldstein, AE (2009). Lipotoxicity in nonalcoholic fatty liver disease: not all lipids are created equal. *Expert Rev Gastroenterol Hepatol* **3**: 445–451.
52. Tamura, Y, Sugimoto, M, Murayama, T, Ueda, Y, Kanamori, H, Ono, K *et al.* (2008). Inhibition of CCR2 ameliorates insulin resistance and hepatic steatosis in db/db mice. *Arterioscler Thromb Vasc Biol* **28**: 2195–2201.
53. Ye, C, Choi, JG, Abraham, S, Wu, H, Diaz, D, Terreros, D *et al.* (2012). Human macrophage and dendritic cell-specific silencing of high-mobility group protein B1 ameliorates sepsis in a humanized mouse model. *Proc Natl Acad Sci USA* **109**: 21052–21057.
54. McArdle, MA, Finucane, OM, Connaughton, RM, McMorrow, AM and Roche, HM (2013). Mechanisms of obesity-induced inflammation and insulin resistance: insights into the emerging role of nutritional strategies. *Front Endocrinol (Lausanne)* **4**: 52.
55. Hotamisligil, GS, Arner, P, Caro, JF, Atkinson, RL and Spiegelman, BM (1995). Increased adipose tissue expression of tumor necrosis factor-alpha in human obesity and insulin resistance. *J Clin Invest* **95**: 2409–2415.
56. Hotamisligil, GS, Shargill, NS and Spiegelman, BM (1993). Adipose expression of tumor necrosis factor-alpha: direct role in obesity-linked insulin resistance. *Science* **259**: 87–91.
57. Hotamisligil, GS, Budavari, A, Murray, D and Spiegelman, BM (1994). Reduced tyrosine kinase activity of the insulin receptor in obesity-diabetes. Central role of tumor necrosis factor-alpha. *J Clin Invest* **94**: 1543–1549.
58. Chen, G and Goeddel, DV (2002). TNF-R1 signaling: a beautiful pathway. *Science* **296**: 1634–1635.
59. de Luca, C and Olefsky, JM (2006). Stressed out about obesity and insulin resistance. *Nat Med* **12**: 41–42; discussion 42.
60. Jager, J, Grémeaux, T, Cormont, M, Le Marchand-Brustel, Y and Tanti, JF (2007). Interleukin-1beta-induced insulin resistance in adipocytes through down-regulation of insulin receptor substrate-1 expression. *Endocrinology* **148**: 241–251.
61. Fasshauer, M, Klein, J, Lossner, U and Paschke, R (2003). Interleukin (IL)-6 mRNA expression is stimulated by insulin, isoproterenol, tumour necrosis factor alpha, growth hormone, and IL-6 in 3T3-L1 adipocytes. *Horm Metab Res* **35**: 147–152.
62. Ruge, T, Lockton, JA, Renstrom, F, Lystig, T, Sukonina, V, Svensson, MK *et al.* (2009). Acute hyperinsulinemia raises plasma interleukin-6 in both nondiabetic and type 2 diabetes mellitus subjects, and this effect is inversely associated with body mass index. *Metabolism* **58**: 860–866.
63. Berg, AH, Combs, TP, Du, X, Brownlee, M and Scherer, PE (2001). The adipocyte-secreted protein Acrp30 enhances hepatic insulin action. *Nat Med* **7**: 947–953.
64. Schwarz, JM, Linfoot, P, Dare, D and Aghajanian, K (2003). Hepatic *de novo* lipogenesis in normoinsulinemic and hyperinsulinemic subjects consuming high-fat, low-carbohydrate and low-fat, high-carbohydrate isoenergetic diets. *Am J Clin Nutr* **77**: 43–50.
65. Brown, MS and Goldstein, JL (2008). Selective versus total insulin resistance: a pathogenic paradox. *Cell Metab* **7**: 95–96.
66. Forsythe, LK, Wallace, JM and Livingstone, MB (2008). Obesity and inflammation: the effects of weight loss. *Nutr Res Rev* **21**: 117–133.
67. Wueest, S, Rapold, RA, Schumann, DM, Rytka, JM, Schildknecht, A, Nov, O *et al.* (2010). Deletion of Fas in adipocytes relieves adipose tissue inflammation and hepatic manifestations of obesity in mice. *J Clin Invest* **120**: 191–202.
68. Kang, YS, Lee, MH, Song, HK, Ko, GJ, Kwon, OS, Lim, TK *et al.* (2010). CCR2 antagonism improves insulin resistance, lipid metabolism, and diabetic nephropathy in type 2 diabetic mice. *Kidney Int* **78**: 883–894.
69. Xia, M and Sui, Z (2009). Recent developments in CCR2 antagonists. *Expert Opin Ther Pat* **19**: 295–303.
70. Struthers, M and Pasternak, A (2010). CCR2 antagonists. *Curr Top Med Chem* **10**: 1278–1298.
71. Sullivan, T, Miao, Z, Dairaghi, DJ, Krasinski, A, Wang, Y, Zhao, BN *et al.* (2013). CCR2 antagonist CCX140-B provides renal and glycemic benefits in diabetic transgenic human CCR2 knockin mice. *Am J Physiol Renal Physiol* **305**: F1288–F1297.
72. Tamura, Y, Sugimoto, M, Murayama, T, Minami, M, Nishikaze, Y, Ariyasu, H *et al.* (2010). C C chemokine receptor 2 inhibitor improves diet-induced development of insulin resistance and hepatic steatosis in mice. *J Atheroscler Thromb* **17**: 219–228.
73. Sullivan, TJ, Miao, Z, Zhao, BN, Ertl, LS, Wang, Y, Krasinski, A *et al.* (2013). Experimental evidence for the use of CCR2 antagonists in the treatment of type 2 diabetes. *Metabolism* **62**: 1623–1632.
74. Di Rocco, P, Manco, M, Rosa, G, Greco, AV and Mingrone, G (2004). Lowered tumor necrosis factor receptors, but not increased insulin sensitivity, with infliximab. *Obes Res* **12**: 734–739.
75. Doyon, J, Coesemans, E, Boeckx, S, Buntinx, M, Hermans, B, Van Wauwe, JP *et al.* (2008). Discovery of potent, orally bioavailable small-molecule inhibitors of the human CCR2 receptor. *ChemMedChem* **3**: 660–669.
76. Si, Y, Tsou, CL, Croft, K and Charo, IF (2010). CCR2 mediates hematopoietic stem and progenitor cell trafficking to sites of inflammation in mice. *J Clin Invest* **120**: 1192–1203.
77. Terwey, TH, Kim, TD, Kochman, AA, Hubbard, VM, Lu, S, Zakrzewski, JL *et al.* (2005). CCR2 is required for CD8-induced graft-versus-host disease. *Blood* **106**: 3322–3330.
78. Chu, HX, Arumugam, TV, Gelderblom, M, Magnus, T, Drummond, GR and Sobey, CG (2014). Role of CCR2 in inflammatory conditions of the central nervous system. *J Cereb Blood Flow Metab* **34**: 1425–1429.
79. Lim, JK, Obara, CJ, Rivollier, A, Pletnev, AG, Kelsall, BL and Murphy, PM (2011). Chemokine receptor Ccr2 is critical for monocyte accumulation and survival in West Nile virus encephalitis. *J Immunol* **186**: 471–478.
80. Poo, YS, Nakaya, H, Gardner, J, Larcher, T, Schroder, WA, Le, TT *et al.* (2014). CCR2 deficiency promotes exacerbated chronic erosive neutrophil-dominated chikungunya virus arthritis. *J Virol* **88**: 6862–6872.
81. Wilcox, DM, Yang, R, Morgan, SJ, Nguyen, PT, Voorbach, MJ, Jung, PM *et al.* (2006). Delivery of RNAi reagents in murine models of obesity and diabetes. *J RNAi Gene Silencing* **3**: 225–236.
82. Leuschner, F, Dutta, P, Gorbatov, R, Novobrantseva, TI, Donahoe, JS, Courties, G *et al.* (2011). Therapeutic siRNA silencing in inflammatory monocytes in mice. *Nat Biotechnol* **29**: 1005–1010.
83. Tesz, GJ, Aouadi, M, Prot, M, Nicoloro, SM, Boutet, E, Amano, SU *et al.* (2011). Glucan particles for selective delivery of siRNA to phagocytic cells in mice. *Biochem J* **436**: 351–362.
84. Jourdan, T, Godlewski, G, Cinar, R, Bertola, A, Szanda, G, Liu, J *et al.* (2013). Activation of the Nlrp3 inflammasome in infiltrating macrophages by endocannabinoids mediates beta cell loss in type 2 diabetes. *Nat Med* **19**: 1132–1140.
85. Novina, CD, Murray, MF, Dykxhoorn, DM, Beresford, PJ, Riess, J, Lee, SK *et al.* (2002). siRNA-directed inhibition of HIV-1 infection. *Nat Med* **8**: 681–686.
86. Howard, KA, Paludan, SR, Behlke, MA, Besenbacher, F, Deleuran, B and Kjems, J (2009). Chitosan/siRNA nanoparticle-mediated TNF-alpha knockdown in peritoneal macrophages for anti-inflammatory treatment in a murine arthritis model. *Mol Ther* **17**: 162–168.
87. Andrikopoulos, S, Blair, AR, Deluca, N, Fam, BC and Proietto, J (2008). Evaluating the glucose tolerance test in mice. *Am J Physiol Endocrinol Metab* **295**: E1323–E1332.

Supplementary Information accompanies this paper on the Molecular Therapy–Nucleic Acids website (http://www.nature.com/mtna)